Article

TRANSPARENT
PROCESS

THE
EMBO
JOURNAL

Guanylyl cyclase-G is an alarm pheromone receptor in mice

Ying-Chi Chao[1], Joerg Fleischer[2,*] (ID) & Ruey-Bing Yang[1,3,4**] (ID)

Abstract

Many animals respond to threats by releasing alarm pheromones (APs) that warn conspecifics. In mice, detection of the AP 2-sec-butyl-4,5-dihydrothiazole (SBT) is mediated by chemosensory neurons residing in the Grueneberg ganglion (GG) of the anterior nasal region. Although the molecular mechanisms underlying activation of GG neurons by SBT and other substances are still unclear, recent studies have reported an involvement of the transmembrane guanylyl cyclase (GC) subtype GC-G in chemosensory signaling in the GG. Here, we show that SBT directly binds with high affinity to the extracellular domain of GC-G and elicits an enhanced enzymatic activity of this protein. In line with this finding, heterologous expression of GC-G renders cells responsive to SBT while activation by SBT was strongly attenuated in GG neurons from GC-G-deficient mice. Consistently, SBT-induced fear-associated behaviors, SBT-evoked elevated blood pressure, and increased serum levels of the stress hormone corticosterone were clearly reduced in GC-G-knockout animals compared to wild-type mice. These observations suggest that GC-G serves as an unusual receptor in GG neurons mediating the detection of the volatile AP substance SBT.

Introduction

Transmembrane guanylyl cyclases (GCs) constitute a unique class of receptor proteins that transmit an extracellular signal directly into the formation of the intracellular second messenger substance cyclic guanosine monophosphate (cGMP). GCs are of critical importance for a number of essential physiological and sensory processes, including blood pressure regulation, cell growth, vision and olfaction (Kuhn, 2009; Potter, 2011). Most of the mammalian transmembrane GCs characterized so far are activated by peptide ligands such as natriuretic peptides, guanylin, or uroguanylin (Kuhn, 2016). Among the seven known murine transmembrane GCs (GC-A through GC-G), subtype GC-G is unusual since its enzymatic activity is stimulated by cool temperatures (Chao *et al*, 2015). Whether GC-G also serves as a receptor protein for chemical ligands is yet unclear although activation of the heterologously expressed intracellular cyclase domain of GC-G by bicarbonate has been reported (Chao *et al*, 2010). With respect to a potential activation of GC-G by chemical ligands, it is important to emphasize that GC-G is strongly expressed in neurons of the so-called Grueneberg ganglion (GG) (Fleischer *et al*, 2009b; Liu *et al*, 2009), a cluster of chemo- and thermosensory cells residing in the anterior nasal regions of mammals (Gruneberg, 1973; Brechbuhl *et al*, 2008, 2013b; Mamasuew *et al*, 2008, 2011a; Schmid *et al*, 2010). Interestingly, responsiveness of GG neurons to given odorants is dependent on GC-G (Mamasuew *et al*, 2011b; Hanke *et al*, 2013), indicating that GC-G might serve as a receptor protein for GG-activating substances.

In recent studies, a small number of chemical compounds have been identified that stimulate GG neurons, including 2-sec-butyl-4,5-dihydrothiazole (SBT) (Mamasuew *et al*, 2011a; Brechbuhl *et al*, 2013b). Among these substances, SBT has been identified as a murine alarm pheromone (AP) eliciting innate fear-related behaviors in mice (Brechbuhl *et al*, 2013b). APs are substances released by an injured or threatened organism to warn conspecifics against danger. For SBT, it has been found recently that this volatile compound is released by mice at estimated concentrations in the micromolar range under given alarm conditions (lethal CO_2 concentrations as well as stressful situations elicited by confinement or cold temperatures) and evokes fear- and stress-associated responses in conspecifics, including freezing, decreased walking distances, and elevated plasma levels of corticosterone (Brechbuhl *et al*, 2013b; Matsuo *et al*, 2015). Yet, the precise mechanisms of SBT synthesis and release in stressful situations are still elusive.

Although the molecular processes mediating detection of APs in mammals are so far largely unknown, detection of SBT and subsequent induction of SBT-evoked defensive and fear-associated

1   Institute of Biomedical Sciences, Academia Sinica, Taipei, Taiwan
2   Department of Animal Physiology, Institute of Biology/Zoology, Martin Luther University Halle-Wittenberg, Halle (Saale), Germany
3   Institute of Pharmacology, School of Medicine, National Yang-Ming University, Taipei, Taiwan
4   Ph.D. Program in Biotechnology Research and Development, College of Pharmacy, Taipei Medical University, Taipei, Taiwan
    *Corresponding author. Tel: +49 345 55 26476; Fax: +49 345 55 27152; E-mail: joerg.fleischer@zoologie.uni-halle.de
    **Corresponding author. Tel: +886 2 2652 3943; Fax: +886 2 2785 8847; E-mail: rbyang@ibms.sinica.edu.tw

responses require a functional GG (Brechbuhl *et al*, 2013b). The latter finding suggests that SBT is received via the olfactory system and that GG neurons are endowed with receptor proteins for the AP substance SBT. However, the precise mechanisms of SBT detection in GG neurons are still elusive. In view of GC-G expression in GG neurons and the ligand-binding properties of other transmembrane GC subtypes that serve as receptors, it was tested whether GC-G might function as a receptor protein for SBT in the GG. The findings of our biochemical and molecular biology approaches as well as Ca^{2+} imaging and behavioral studies strongly indicate that SBT is a ligand for the orphan receptor GC-G in the GG, demonstrating that transmembrane GCs are not only activated by peptide ligands but also by low molecular weight substances. Moreover, the present results provide first insights into the molecular mechanism underlying detection of the AP substance SBT.

Results

SBT stimulates GC-G enzymatic activity

To explore whether GC-G might function as a receptor protein for the murine AP substance SBT, we first investigated whether the cyclase activity of GC-G is affected by SBT in a heterologous expression system. For this purpose, HEK-293T cells were transiently transfected with a plasmid encoding full-length (FL) GC-G

or a truncated GC-G isoform lacking a substantial portion of the extracellular domain (ΔECD) (Fig 1A). Subsequently, cells were harvested and incubated [in the presence of the phosphodiesterase inhibitor 3-isobutyl-1-methylxanthine (IBMX)] with different concentrations of SBT (0, 250, or 500 nM). The results shown in Fig 1B demonstrate that SBT indeed stimulated in a dose-dependent manner intracellular cGMP accumulation in HEK-293T cells expressing GC-G FL. In cells transfected with an empty vector, SBT did not increase cGMP concentration. A dose-dependent activation of GC-G enzymatic activity by SBT was also observed when membrane protein fractions isolated from HEK-293T cells expressing GC-G FL were used to monitor cyclase activity (in the presence of IBMX) (Fig 1C). Such a SBT-evoked increase in the cGMP synthesis was not detectable in membrane fractions from HEK-293T cells transfected with an empty vector, indicating that GC-G renders cells responsiveness to SBT.

In control experiments, to assess the specificity of GC-G activation by SBT, two other odorous compounds (butyric acid and 2-heptanone) that do not activate GG neurons (Mamasuew *et al*, 2011a; Brechbuhl *et al*, 2013b) were tested for their potential to stimulate GC-G enzymatic activity. In contrast to SBT, these two

Figure 1. SBT specifically stimulates the enzymatic activity of GC-G dependent on the presence of the extracellular domain.

A Schematic representation of the domain structure of full-length (FL) GC-G and its mutant variant lacking the extracellular domain (ΔECD) (modified from Chao *et al*, 2015). SP, signal peptide sequence; ECD, extracellular domain; TM, transmembrane region; KLD, kinase-like domain; CYC, cyclase catalytic domain.

B, C SBT stimulates intracellular cGMP accumulation and GC activity in a dose-dependent manner. Two days after transient transfection with an empty vector or a plasmid coding for GC-G FL, HEK-293T cells were incubated for 20 min with the indicated concentrations of SBT and cellular cGMP concentration was measured (B). In addition, membrane preparations from HEK-293T cells transfected with an empty vector or a plasmid encoding GC-G FL were utilized to determine GC activity during a 20-min interval at the indicated concentrations of SBT (C).

D, E Deletion of the extracellular domain of GC-G abolishes the stimulatory effect evoked by SBT. Two days after transient transfection of HEK-293T cells with a plasmid coding for the FL or the ΔECD variant of GC-G, transfected cells (D), or membrane fractions isolated from these cells (E) were treated with SBT (500 nM) for 20 min to measure cellular cGMP concentration (D) or GC activity (E), respectively. For control experiments, the reaction buffer was not supplemented with SBT but only with the solvent dimethyl sulfoxide (DMSO).

F GC-G is the only transmembrane GC subtype activated by SBT. HEK-293T cells were transfected with an empty vector or plasmids encoding the FLAG-tagged murine GC subtypes GC-A to GC-G. Two days after transient transfection, cellular cGMP concentrations were measured upon exposure to 500 nM SBT for 20 min (upper panel). For control experiments, the reaction buffer was not supplemented with SBT but only with the solvent DMSO. Expression of transmembrane GCs was monitored by Western blotting using an anti-FLAG antibody (lower panel).

Data information: All data are mean ± SD from three experiments in triplicate; two-tailed *t*-test **P < 0.01.
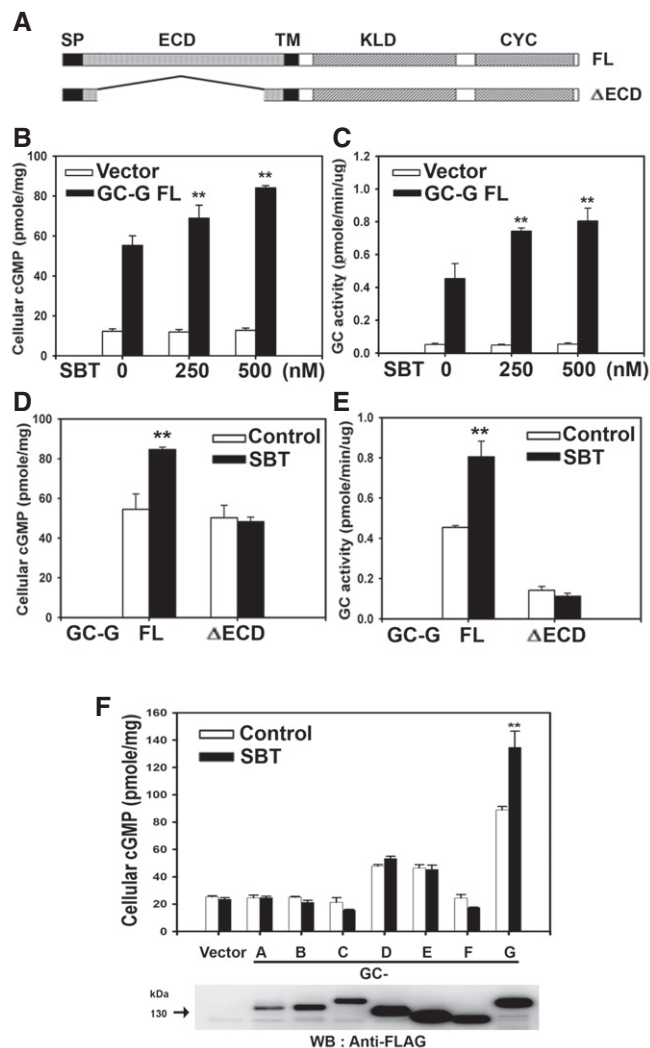
compounds did not affect the intracellular cGMP accumulation in HEK-293T cells expressing GC-G FL (Appendix Fig S1).

The extracellular domain of GC-G is essential for stimulation by SBT

Transmembrane GCs are proteins with a single transmembrane domain separating an N-terminal extracellular domain (ECD) and an intracellular region; the latter comprises a protein kinase-like domain (KLD) and a C-terminal cyclase catalytic domain (CYC) (Fig 1A) (Kuhn, 2016). To scrutinize whether the ECD that is critical for ligand binding in other transmembrane GCs (Potter, 2011) might be involved in SBT-evoked activation of GC-G, we compared the effect of SBT on GC-G FL and the above-mentioned mutant GC-G protein lacking the ECD (ΔECD) (Fig 1A). While expression and cell surface targeting were similar for both GC-G variants (FL and ΔECD) (data not shown), for the ΔECD variant, the SBT-induced cGMP accumulation in HEK-293T cells (Fig 1D) and in membrane preparations obtained from these cells (Fig 1E) was completely abolished. Consequently, in marked contrast to HEK-293T cells and the corresponding membrane fractions endowed with GC-G FL, cGMP synthesis in samples with the ΔECD variant was not elevated upon addition of SBT compared to controls lacking SBT. This failure of SBT to stimulate the enzymatic activity of the ΔECD variant is most likely due to abolishment of SBT binding to GC-G in the absence of the ECD. However, it cannot be ruled out entirely that elimination of the ECD might severely affect the ability of GC-G to synthesize cGMP. To address this issue, we have conducted additional experiments to assess whether the ΔECD variant of GC-G is still capable of stimulated cGMP synthesis. In this context, it has been reported previously that similar to other transmembrane GCs, Mn^{2+} or Mn^{2+} and Triton X-100 increased the enzymatic activity of GC-G (FL variant) (Kuhn *et al*, 2004). In fact, the cyclase activity of the mutant GC-G protein lacking the ECD was clearly stimulated in the presence of Mn^{2+} or Mn^{2+} and Triton X-100, respectively (Appendix Fig S2A). In addition to activation by Mn^{2+} or Mn^{2+} and Triton X-100, GC-G enzymatic activity has been recently found to be stimulated by cool temperatures (Chao *et al*, 2015). Similar to GC-G FL, cGMP accumulation in HEK-293T cells expressing the truncated isoform of GC-G lacking the ECD was largely increased at a cool ambient temperature (Appendix Fig S2B), indicating that this mutant protein can be stimulated to produce cGMP by coolness. Collectively, these data demonstrate that the ΔECD variant of GC-G has retained its capacity to generate cGMP. Finally, SBT did not stimulate GC activity in membrane preparations from HEK-293T cells expressing the other members (GC-A to GC-F) of the transmembrane GC family (Fig 1F). In summary, these results demonstrate that SBT specifically stimulates the activity of GC-G and that the ECD of GC-G is critical for the SBT-induced activation.

Expression of GC-G and CNGA3 confers SBT responsiveness to HEK cells

In neurons of the GG, responsiveness to the odorant 2,3-dimethylpyrazine is dependent on the expression of GC-G and the cGMP-activated ion channel CNGA3 (Mamasuew *et al*, 2011b; Hanke *et al*, 2013). To assess if these signaling elements render cells responsive to the AP compound SBT and to further evaluate whether GC-G

could thereby serve as a receptor protein for this substance, HEK-293T cells heterologously expressing CNGA3 and GC-G were loaded with the Ca^{2+}-sensitive dye Fura-2 and used for ratiomeric calcium imaging experiments. In HEK-293T cells co-expressing CNGA3 and GC-G FL, the intracellular Ca^{2+} concentration increased upon exposure to SBT in a dose-dependent manner (Fig 2A). By contrast, in HEK-293T cells expressing only CNGA3 or CNGA3 along with the truncated variant of the GC-G protein lacking the ECD (GC-G ΔECD), the intracellular Ca^{2+} concentration was not substantially affected by exposure to SBT (Fig 2B and C). These findings further
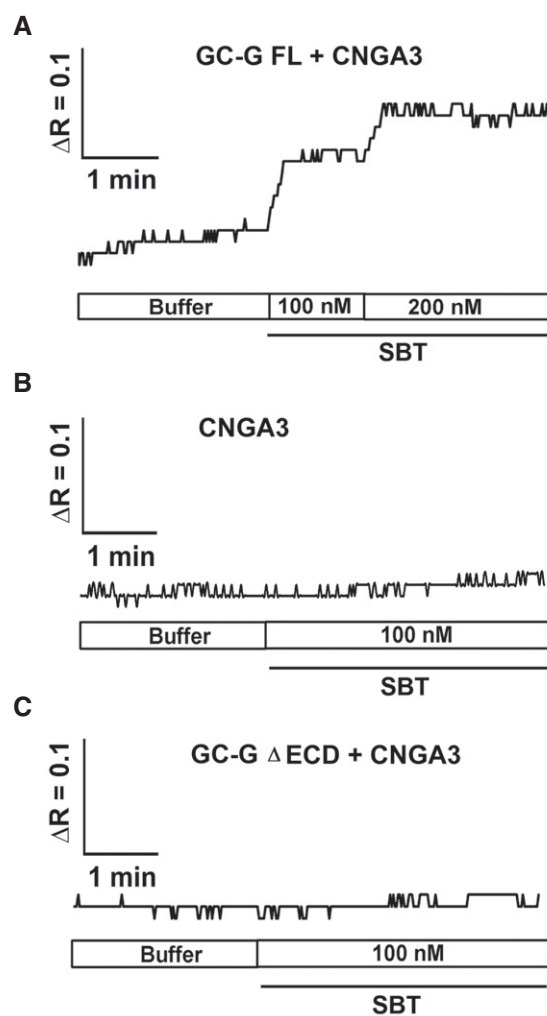
Figure 2. SBT-induced rise of the intracellular calcium $[Ca^{2+}]_i$ concentration in HEK-293T cells upon co-expression of full-length GC-G and CNGA3.

A   Incubation of cells co-expressing GC-G FL and CNGA3 with SBT led to a dose-dependent increase in $[Ca^{2+}]_i$. Changes in the ratio of the fluorescence intensity of Fura-2 at 340/380 nm excitation are given by ΔR.

B, C   Treatment with SBT did not increase intracellular Ca^{2+} concentrations in cells expressing only CNGA3 or CNGA3 along with the ΔECD variant of GC-G.

Data information: The Ca^{2+} responses depicted in (A–C) are representative of 30 cells recorded from three experiments.

support the concept that the ECD is critical for SBT-induced stimulation of GC-G. Moreover, these observations demonstrate that GC-G and CNGA3 are sufficient to render cells responsive to SBT.

Direct binding of SBT to the ECD of GC-G

Although GC-G activation by bicarbonate has been reported (Chao *et al*, 2010), to our knowledge, no GC-G-binding ligand has been identified so far. Based on the above-mentioned observation that the ECD of GC-G is required for SBT-induced GC-G activation, surface plasmon resonance (SPR) spectroscopy (Papalia *et al*, 2006; Chu *et al*, 2014; Yang *et al*, 2014) was utilized to examine whether SBT could act as a ligand that directly binds to the ECD of GC-G. Thereby, a powerful SPR instrument (Biacore T200) was used to monitor real-time and label-free small-molecule/protein interactions and to determine their binding affinity. For this approach, the putative ligand-binding ECD of GC-G (residues 44–472) was expressed as human IgG1 Fc fusion protein (GC-G-ECD.Fc) (Fig 3A) to facilitate the purification process and to generate a dimeric receptor [the latter aspect is of particular relevance since transmembrane GCs are generally supposed to form homodimers (Kuhn, 2016)]. The results showed that SBT indeed binds to the ECD of GC-G with high affinity (K_D = 78.3 ± 17.2 nM) (Fig 3B and C). Thus, these data support the view that SBT is a ligand for GC-G. Using the same experimental approach, potential binding of two other odorous compounds (butyric acid and 2-heptanone) to the ECD of GC-G was tested to assess its ligand specificity. In marked contrast to SBT, in these experiments, butyric acid and 2-heptanone did not bind to the ECD of GC-G (Appendix Fig S3).

Reduced responsiveness to SBT in GG neurons from GC-G-deficient mice

SBT-induced responses in GG neurons can be monitored by recording the intracellular Ca^{2+} concentration (Brechbuhl *et al*, 2013b). To assess the relevance of GC-G for the responsiveness of GG neurons to SBT, ratiometric Ca^{2+} imaging experiments were performed on tissue slices through the GG. For this purpose, appropriate tissue slices from OMP-GFP or OMP-GFP/GC-G-KO mouse pups were used and perfused with recording buffer at 37°C. In these mouse strains, GG neurons fluoresce in green (as shown for an OMP-GFP mouse in Fig 4A) based on the expression of the green fluorescent protein (GFP) as a reporter under control of the promoter for the olfactory marker protein (OMP) (Chao *et al*, 2015). In Ca^{2+} imaging experiments, addition of SBT to the recording buffer induced a substantial calcium signal in 24 out of 30 (~80%) tested GFP-positive GG neurons from OMP-GFP mice (three slices from different animals) (Fig 4B). Only six of these 30 GG neurons did not respond to SBT (Appendix Fig S4; lower row). By contrast, examining GFP-positive GG neurons from OMP-GFP/GC-G-KO mice, SBT-induced calcium signals were only detectable in six out of 32 tested cells (< 20%). In the overwhelming majority (26 of 32) of the GG neurons analyzed from these animals, no response to SBT was observed (three slices from different animals) (Fig 4C). Even in the six GG neurons from OMP-GFP/GC-G-KO mice responding to SBT, signals were weaker and more delayed in comparison with SBT-activated GG cells from animals with functional GC-G (Appendix Fig S4; upper row). Thus, the average SBT-induced calcium signal was significantly lower in GG neurons from GC-G-deficient mice compared to GG neurons from

A

B

C
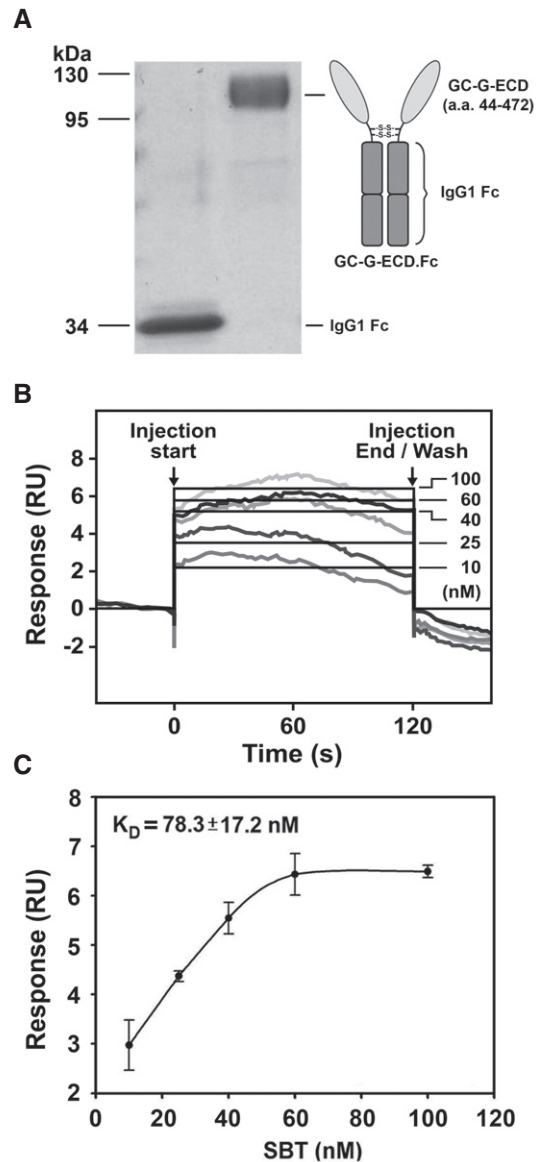
Figure 3. Direct binding of SBT to the ECD of GC-G.

A   The left panel shows a protein gel loaded with purified recombinant GC-G-ECD.Fc protein following electrophoresis and staining with Coomassie Blue. The domain structure of the recombinant GC-G-ECD.Fc protein is depicted in the right panel. This recombinant protein contains the extracellular domain of GC-G (amino acids 44–472) fused with human IgG1 Fc domain. Disulfide bridges cross-linking the Fc subunits are indicated (S-S).

B   Raw data from surface plasmon resonance (SPR) spectroscopy experiments upon SBT injections. The SBT concentrations used in these approaches are given. The black lines represent the global fit of the data to a 1:1 biomolecular interaction model. Responses are indicated in relative units (RU).

C   Determination of the equilibrium dissociation constant (K_D) via analyses of sensorgrams and kinetic fitting. The K_D was derived by the simplest 1:1 binding model. The K_D was determined based on three experiments. Data are mean ± SD from three experiments in duplicate.

conspecifics expressing functional GC-G (Fig 4D). However, upon exposure to potassium chloride (KCl), responses were also observed in GG neurons from GC-G-deficient mice, demonstrating viability of
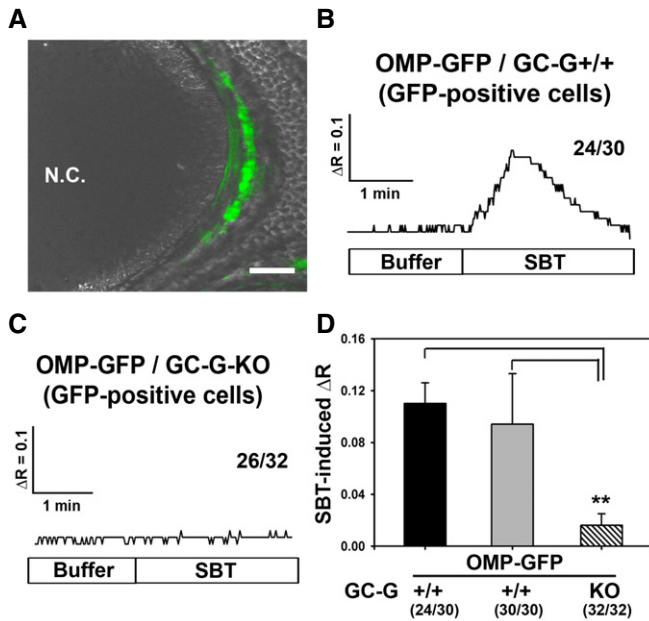
Figure 4. Reduction in SBT-evoked Ca²⁺ responses in GG neurons of GC-G-KO mice.

A   Microscopical image of a tissue slice through the GG of an OMP-GFP pup. GG neurons are labeled in green due to intrinsic GFP fluorescence (GFP fluorescence was merged with the transmitted-light channel). N.C., nasal cavity. Scale bar: 50 μm.

B, C   Representative ratiometric Ca²⁺ transients following exposure to SBT (1 μM) in GFP-positive GG neurons from OMP-GFP/GC-G⁺/⁺ (B) and OMP-GFP/GC-G-KO (C) pups. The numbers on the right-hand side represent the number of cells with Ca²⁺ transients similar to what is shown in the respective graph over the total number of measured cells. For OMP-GFP/GC-G⁺/⁺ or OMP-GFP/GC-G-KO mice, the GG neurons originated from three slices (obtained from different animals).

D   Quantification of SBT-evoked ΔR in GG neurons from OMP-GFP/GC-G⁺/⁺ and OMP-GFP/GC-G-KO mice. SBT-induced ΔR was calculated by subtracting the baseline fluorescence ratio (340/380 nm) at 37°C in the absence of SBT from the peak fluorescence ratio measured upon exposure to SBT. For OMP-GFP/GC-G⁺/⁺, the black bar indicates SBT-evoked ΔR for the 24 SBT-responsive GG neurons, while the gray bar denotes SBT-induced ΔR for all 30 analyzed GG neurons from three slices (obtained from different animals). For OMP-GFP/GC-G-KO, the shaded bar indicates SBT-evoked ΔR for 32 GG neurons analyzed from three slices (obtained from different animals). Data are mean ± SD; two-tailed *t*-test **$P < 0.01$.

these cells (data not shown). In summary, these results reveal that genetic ablation of GC-G greatly compromises responsiveness to SBT in the GG, suggesting that GC-G significantly contributes to SBT-induced GG responses.

**Attenuation of SBT-induced reactions related to fear and stress in GC-G-KO mice**

Previously, SBT has been shown to stimulate GG neurons and to elicit a number of innate fear- and stress-associated responses in mice, including freezing, a decrease in walking distance and increased plasma levels of the rodent stress hormone corticosterone (Brechbuhl *et al*, 2013b; Matsuo *et al*, 2015). To evaluate a functional relevance of GC-G for such SBT-induced reactions, walking
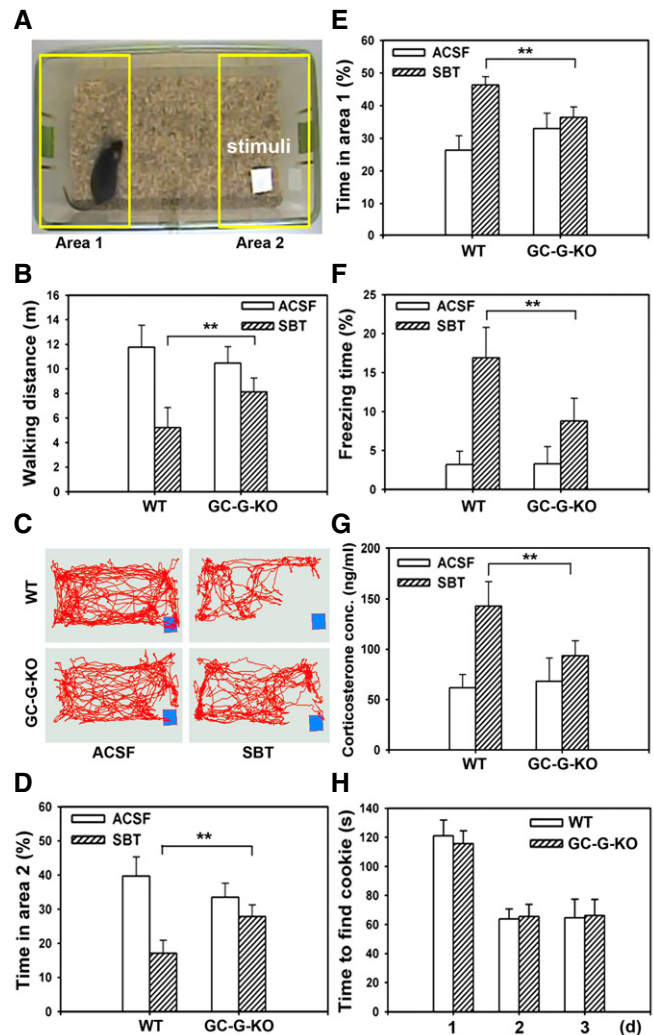
Figure 5. Attenuation of SBT-evoked innate fear and stress responses in GC-G-KO mice.

A   Example of a video frame demonstrating the behavioral assay in which a male mouse (only male mice were used) was exposed to a piece of blotting paper impregnated with SBT (stimulus) or ACSF buffer (control). Behavioral experiments involving adult WT and GC-G KO mice (8 weeks old) were exposed successively for 5 min to SBT.

B   In the presence of SBT, the walking distance [measured in meters (m)] was significantly higher in GC-G-KO than in WT mice.

C   Traces reflecting all positions along the trajectory that a representative WT or GC-G-KO mouse traveled in the testing chamber during a 5-min session in the presence of SBT or ACSF (control). The position of the blotting paper soaked with either SBT or ACSF is indicated by the blue rectangle.

D, E   Percentage of time spent by WT and GC-G-KO mice in each of the two opposite cage areas [area 1 (E) and area 2 (D) are circumscribed by the yellow rectangles in (A)] in the presence of SBT or ACSF.

F   In the presence of SBT, the percentage of freezing time was decreased in GC-G-KO mice as compared to WT animals.

G   SBT-evoked elevation of the plasma concentration of the stress hormone corticosterone was impaired in GC-G-KO mice as compared to WT conspecifics.

H   The time [measured in seconds (s)] required to find a hidden cookie was not affected in GC-G-KO mice. For each genotype, six animals were tested. Experiments were conducted on three subsequent days (d).

Data information: Data are mean ± SD; two-tailed *t*-test **$P < 0.01$. For each genotype, six animals were tested.
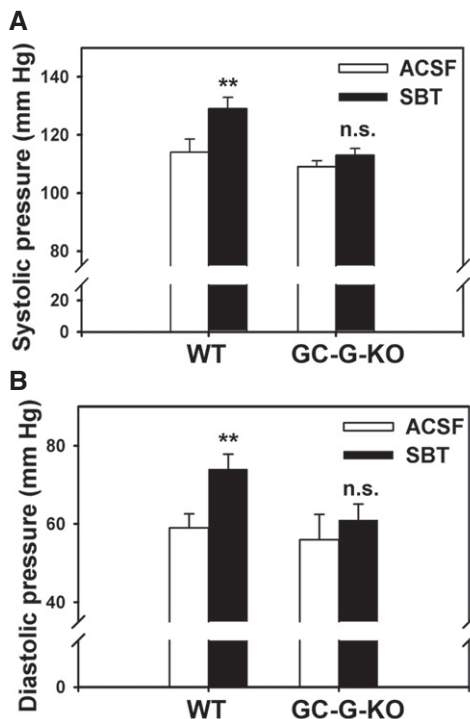
Figure 6. SBT-stimulated elevation of blood pressure is impaired in GC-G-KO mice.

A, B   The blood pressure of mice was measured by a rapid and non-invasive tail-cuff approach. Using magnetic restrainers, adult mice (8 weeks old) were held on a tail-cuff platform connected to a control unit and a computer. The blood pressure was measured continuously, starting with three control sessions (exposure to ACSF) followed by three test sessions (exposure to SBT). Each session contained 10 successive measurements. Upon exposure to SBT, both systolic (A) and diastolic (B) pressures were significantly increased in WT but not in GC-G KO mice. For each genotype, six animals were analyzed. Data are mean ± SD; two-tailed *t*-test. n.s., not significant; **$P < 0.01$.

distance, freezing, and avoidance behavior as well as serum corticosterone concentrations were monitored upon exposure to SBT, comparing wild-type (WT) and GC-G-KO mice (Fig 5). For this purpose, a piece of blotting paper supplemented with either SBT (1% in DMSO) or (as a control) ACSF (artificial cerebrospinal fluid) was placed into one corner of a cage (Fig 5A). Subsequently, walking and freezing of mice in this cage were recorded. These approaches revealed that there was no clear difference concerning the walking distance between WT and GC-G-KO animals upon exposure to ACSF. However, in the presence of SBT, the walking distance was significantly lower in WT than in GC-G-KO animals (WT = 5.2 ± 1.6 m, $n = 6$ versus GC-G-KO = 8.1 ± 1.1 m, $n = 6$; $P < 0.01$), indicating that the SBT-evoked reduction in walking distance is attenuated upon elimination of GC-G (Fig 5B). Tracking the walking also demonstrated that the corner harboring the blotting paper soaked with SBT was avoided (Fig 5C and Appendix Fig S5). In this context, detailed analyses showed that WT animals spent less time in the cage area with the blotting paper (area 2, Fig 5D), in case this paper was impregnated with SBT. In comparison, in the presence of SBT, the time spent in this area by GC-G-KO mice was

significantly higher (Fig 5D), indicating that avoidance of SBT is reduced in GC-G-deficient animals. Conversely, the time spent in area 1 (the area on the opposite side of the cage, Fig 5A) was clearly decreased in GC-G-KO versus WT animals when the blotting paper was soaked with SBT (Fig 5E). Upon exposure to SBT, the freezing time was increased in both WT and GC-G-KO mice. Yet, SBT-evoked freezing (the percentage of freezing time) was significantly lower in GC-G-deficient animals (WT = $16.9 \pm 3.9\%$, $n = 6$ versus GC-G-KO = $8.8 \pm 2.9\%$, $n = 6$; $P < 0.01$) (Fig 5F). Comparing the walking distance and the freezing time with animals exposed to ACSF (control), in marked contrast to SBT (dissolved in DMSO) (Fig 5B and F), DMSO alone did not significantly affect walking and freezing behavior of WT mice (Appendix Fig S6). Finally, analyzing the release of stress hormones, blood serum concentrations of corticosterone were similar in WT and GC-G-KO mice exposed to ACSF. However, the SBT-evoked increase in corticosterone concentrations was diminished in animals lacking GC-G (Fig 5G). In summary, these findings indicate that SBT-induced responses related to fear and stress are reduced in GC-G-deficient mice. To assess the capacity of GC-G-KO mice to generally detect odors, the ability to localize a hidden Oreo cookie (Brechbuhl *et al*, 2013b) was tested. It was observed that GC-G-deficient mice are capable of finding hidden cookies as quick as WT conspecifics (Fig 5H), suggesting that elimination of GC-G does not generally affect the detection of odors.

Because GG activation by SBT evokes reactions associated with fear and stress in mice (Brechbuhl *et al*, 2013b), we next analyzed whether SBT might also affect blood pressure in a GC-G-dependent manner since acute stress has been reported to increase arterial blood pressure in mice (Farah *et al*, 2004; Takahashi, 2014; Brechbuhl *et al*, 2015). In fact, exposure to SBT elicited a significant rise of both systolic and diastolic blood pressure in WT mice, whereas SBT failed to substantially increase systolic (Fig 6A) and diastolic (Fig 6B) blood pressure in GC-G-KO animals.

Discussion

The murine GG is considered as a chemosensory organ detecting alerting chemical compounds originating from conspecifics or carnivorans, including the alarm pheromone (AP) substance SBT as well as predator scents (Mamasuew *et al*, 2011a; Brechbuhl *et al*, 2013b, 2015). In nasal chemosensory tissues, odorous and pheromonal compounds are supposed to activate sensory neurons via olfactory receptor proteins that reside in the membrane of these cells and belong to various groups of G protein-coupled receptors (Fleischer *et al*, 2009a). In the GG, in spite of considerable efforts, expression of only a few olfactory receptors has been observed so far. Moreover, expression of these receptors in the murine GG seems to mainly occur in development stages around birth (Fleischer *et al*, 2006, 2007). Thus, the receptors enabling GG neurons to respond to APs or predator-derived odorants remained elusive. Importantly, for some GG-activating compounds (notably pyrazine derivatives), it has been observed recently that stimulation of GG neurons is reduced in GC-G-deficient mice, suggesting that the transmembrane GC subtype GC-G, which is expressed in numerous GG cells, plays a pivotal role in the chemo-electrical transduction process (Mamasuew *et al*, 2011b; Hanke *et al*, 2013). Regarding their functional relevance for mammalian cells, transmembrane GCs are

generally considered to serve as receptor proteins for specific ligands. Therefore, in the present study, we set out to assess whether SBT, a substance strongly activating GG neurons (Brechbuhl *et al*, 2013b), might function as a cognate ligand for GC-G. Our experimental approaches have shown that SBT stimulates GC-G enzymatic activity in cell cultures and in membrane protein fractions (Fig 1) while SBT-induced responses in GG neurons from GC-G-deficient mice were considerably decreased (Fig 4D). Moreover, upon expression of (full-length) GC-G, cells become responsive to GC-G (Fig 2). These findings suggest that GC-G indeed serves as a receptor for SBT. The experiments of the present study also demonstrate that GC-G binds SBT via its ECD with high affinity (Figs 1D and E, 2C, and 3). This observation is remarkable since other transmembrane GCs have been previously reported to only bind peptide ligands via their ECD (Kuhn, 2016). Thus, to our knowledge, this is the first time that the ECD of a transmembrane GC has been found to bind a small-molecule ligand. Accordingly, other transmembrane GCs might be also capable of interacting with non-peptide ligands via their ECD. This is particularly relevant for given GC subtypes for which no extracellular ligand has been identified so far (Kuhn, 2016). In this context, GC-G could also serve as a receptor for other small-molecule ligands (most notably heterocyclic compounds originating from predator urine or feces) that activate GG neurons and affect murine behavior (Mamasuew *et al*, 2011a; Brechbuhl *et al*, 2013b, 2015). Moreover, the activation of GC-G by the small-molecule ligand SBT raises the possibility that chemically related or unrelated small-molecule ligands might stimulate the enzymatic activity of GC-G in cell types distinct from GG neurons, including kidney and sperm cells that have been reported to express GC-G as well (Kuhn *et al*, 2004; Lin *et al*, 2008).

In addition to odorous or pheromonal compounds (such as SBT), GG neurons are also activated by cool temperatures (Mamasuew *et al*, 2008; Schmid *et al*, 2010). In this regard, it is important to note that GC-G functions in GG neurons as a "dual receptor" for chemical ligands (SBT; this study) and coolness (Chao *et al*, 2015). However, the "dual sensitivity" of GC-G for chemicals and noxious temperatures is not unique but reminiscent of certain transient receptor potential (TRP) ion channels, which are also activated by noxious temperatures and specific chemical compounds. These TRP channel subtypes (most notably TRPV1, TRPM8 and TRPA1) are expressed in thermosensory and nociceptive somatosensory neurons and respond to noxious hot or cold temperatures as well as to irritant substances including capsaicin (from chili pepper), menthol or mustard oil (Vay *et al*, 2012). Thus, in analogy to nociceptive neurons using "dual receptors" (TRP channels) for detecting noxious temperatures and potentially harmful chemicals, GG neurons utilize the "dual receptor" GC-G for reception of unpleasant cool temperatures and the AP substance SBT indicating danger. Moreover, similar to GC-G, the protein domains mediating activation of these TRP channels by given temperatures on the one hand and chemical ligands on the other hand are not identical (Brauchi *et al*, 2006). For GC-G, the ECD is strictly necessary to bind SBT (Figs 1D and E, 2C, and 3) and binding of SBT to the ECD of GC-G appears to be highly specific since other transmembrane GC subtypes are not activated by SBT (Fig 1F). In contrast, the ECD of GC-G is dispensable for activation by coolness, which mostly relies on intracellular domains (Chao *et al*, 2015). It remains unclear why GG neurons utilize a "dual receptor" instead of two distinct

receptors to detect different modalities. Taking into consideration that cool temperatures enhance GG responsiveness to given chemicals (Mamasuew *et al*, 2011a; Brechbuhl *et al*, 2013a), GC-G might serve as an interface that facilitates crosstalk between thermo- and chemosensory signaling in the GG.

In mice, 2-sec-butyl-4,5-dihydrothiazole [SBT (also designated as DHT)] has been initially reported as a pheromone that is specifically present in male urine and elicits inter-male aggression, investigatory sniffing from female mice and contributes to more frequent estrous cycles in females (Jemiolo *et al*, 1985; Novotny *et al*, 1985; Schwende *et al*, 1986). In a more recent study, however, SBT has been proposed as an AP in mice that is released under alarm conditions (increased CO_2 concentration or stress situations) by both males and females and elicits innate fear- and stress-associated responses, including freezing, decreased walking distances and elevated plasma levels of corticosterone (Brechbuhl *et al*, 2013b; Matsuo *et al*, 2015). The findings of the present study (Fig 5) largely substantiate the latter concept, confirming that SBT acts as an AP. It is yet elusive how SBT can promote sex-specific responses [inter-male aggression, investigatory sniffing from females and more frequent estrous cycles (Jemiolo *et al*, 1985; Novotny *et al*, 1985)] as well as responses related to fear and stress. In this regard, detection of SBT via different olfactory organs might be important. In fact, SBT does not only stimulate GG cells but also affects chemosensory neurons in the vomeronasal organ and in the main olfactory epithelium (Zhou & Moss, 1997; Moss *et al*, 1998). It is therefore conceivable that under non-alarm conditions, when SBT release from mice is comparatively low (Brechbuhl *et al*, 2013b), only chemosensory neurons in the vomeronasal organ and/or the main olfactory epithelium are affected. By contrast, a considerable increase in the SBT release from mice under alarm conditions (Brechbuhl *et al*, 2013b) would also activate SBT-sensitive GG neurons. Consequently, the (additional) activation of GG neurons at elevated SBT concentrations might turn off the above-mentioned SBT-induced sex-specific responses and elicit SBT-evoked stress- and fear-associated responses via the GG. Accordingly, in the murine nose, there might be differential sensitivities for SBT between distinct chemosensory organs. This could be due to different receptors with divergent affinity for SBT. While GC-G serves as receptor for SBT in the GG (this study), GC-G is absent from the vomeronasal organ and the main olfactory epithelium (Fleischer *et al*, 2009b). Consequently, other receptor proteins must be relevant for SBT detection in these nasal compartments. This scenario is reminiscent of the previously described reception of overlapping sets of pheromones in the vomeronasal organ and the main olfactory epithelium via divergent signaling pathways (Spehr *et al*, 2006).

With respect to the reception of pheromonal substances, as a member of the GC family, GC-G appears to be an unusual receptor since pheromones are supposed to be detected via more "canonical" olfactory receptor proteins, including odorant and vomeronasal receptors that belong to the large superfamily of G protein-coupled receptors (Fleischer *et al*, 2009a; Spehr & Munger, 2009). However, GC-G is not the only transmembrane GC subtype serving as olfactory receptor. In a subset of sensory neurons in the main olfactory epithelium, the GC subtype GC-D functions as an olfactory receptor protein mediating the reception of guanylin and uroguanylin as well as CO_2 and CS_2 (Hu *et al*, 2007; Leinders-Zufall *et al*, 2007; Duda & Sharma, 2008; Munger *et al*, 2010). Because the

peptides guanylin and uroguanylin are excreted in mouse urine and feces (Forte, 2004; Valentino *et al*, 2011) and promote the acquisition of food preferences in conspecifics (Arakawa *et al*, 2013), GC-D can be considered as a pheromone receptor as well. Thus, the two GC subtypes GC-D and GC-G expressed in chemosensory tissues seem to be both dedicated to the detection of pheromones.

The concept that the GG functions as a detector for APs was mainly based on two observations in earlier studies. First, the AP substance SBT activated GG neurons. Second, in juvenile mice subjected to incisions of nasal tissue with a needle (0.46 mm thick), due to axotomy of GG axons, the GG degenerated and SBT-induced behavioral as well as physiological responses were lost or at least largely reduced (Brechbühl *et al*, 2008, 2013b). The latter aspect is critical because it cannot be ruled out that the diminished responses to SBT observed in axotomized mice might be due to damaging of other chemosensory structures in the nose (including other olfactory organs or the trigeminal nerve) during incisioning with such a thick needle. The finding of the present study that GC-G serves as receptor for SBT allowed us to use GC-G-deficient mice to analyze whether the GG indeed functions as a chemodetector important for eliciting behaviorally and physiologically relevant responses via the AP substance SBT. In the head of mice, GC-G is specifically expressed in GG neurons and is therefore absent from other chemosensory organs in the nose (Fleischer *et al*, 2009b; Chao *et al*, 2015). Consequently, the observed significant attenuation of SBT-induced innate fear- and stress-related responses in GC-G-KO mice (Figs 5 and 6) strongly supports the concept that the GG is essential for mediating such SBT-evoked responses. Thus, GC-G-KO mice might be an attractive model organism to study the behaviors and physiological processes induced by the AP substance SBT and the involvement of the GG in these SBT-evoked responses. In GC-G-KO animals, however, a few GG neurons were also activated by SBT (Fig 4D and Appendix Fig S4), suggesting that GC-G may not be the only receptor responsible for SBT detection in the GG. In fact, expression of several olfactory receptors in GG neurons has been demonstrated (Fleischer *et al*, 2006, 2007). Whether SBT activates one of these receptors in addition to GC-G is currently unknown.

Materials and Methods

Cell culture, transfection, generation of expression plasmids, membrane fraction isolation, GC activity assay, immunoprecipitation, and Western blotting

These experimental approaches were performed as described previously (Kuhn *et al*, 2004; Chao *et al*, 2015).

Reagents

All chemicals were of high purity (reagent grade) and purchased from Sigma-Aldrich (St. Louis, MO, USA). Anti-FLAG M2 monoclonal antibodies as well as anti-FLAG M2 covalently attached to agarose were also purchased from Sigma-Aldrich. 2-sec-butyl-4,5-dihydrothiazole (SBT) was synthesized as described previously (Lehman-McKeeman *et al*, 1998) or purchased from Tractus (London, UK). The purity of SBT was over 88% as determined by gas chromatography. For calcium imaging approaches and

experiments investigating GC-G activity, SBT was dissolved in dimethyl sulfoxide (DMSO). Subsequently, the SBT/DMSO solution was diluted 1,000-fold using an appropriate buffer solution, leading to the desired final concentration of SBT and a final concentration of DMSO of 0.1%. In the experiments investigating behaviors and physiological reactions associated with fear and/or stress, SBT was diluted to a final concentration of 1% in DMSO.

Construction of expression plasmids

The FLAG-tagged GC-G [full-length (FL)] expression plasmid (FLAG.GC-G FL) was constructed as detailed previously (Chao *et al*, 2010). Expression plasmids encoding FLAG-tagged GC-A to GC-F were constructed similarly using the pFLAG-CMV1 vector (Sigma-Aldrich). The FLAG-tagged ΔECD variant lacks the extracellular domain of GC-G (residues 44–472). The GC-G-ECD.Fc construct contains only the ECD of GC-G fused with human IgG$_1$ Fc fragment at the C-terminus.

SPR binding assay

The interaction analyses were performed using SPR technology on a Biacore T200 instrument (GE Healthcare, Pittsburgh, PA, USA) (Papalia *et al*, 2006; Chu *et al*, 2014; Yang *et al*, 2014). Briefly, the GC-G-ECD.Fc fusion protein (50 μg/ml) was purified using protein A agarose and captured by the Series S CM5 Sensor chip pretreated with Human Antibody Capture Kit (GE Healthcare). A series of SBT, butyric acid, and 2-heptanone concentrations were prepared in PBS running buffer containing 0.1% DMSO and injected at a flow rate of 50 μl/min for 3 min over the CM5 chip. Experiments were carried out at 25°C. Sensorgrams of SBT were analyzed to obtain kinetic data and affinities (including the dissociation constant K_D and the associated constant K_A) using Biacore T200 Evaluation Software (Version 2.0; GE Healthcare). The K_D was derived by the simplest 1:1 binding model.

Mouse strains

This study was performed with littermates of wild-type (WT) and the GC-G-knockout (GC-G-KO) mice derived from heterozygous intercrosses in C56BL/6 background (Chao *et al*, 2015). In the OMP-GFP transgenic mouse line, green fluorescence protein (GFP) is expressed as a reporter under control of the olfactory marker protein (OMP) promoter. In these transgenic mice, the coding sequence of the OMP gene and 150 nucleotides of the 3′ noncoding region are replaced by a GFP-encoding sequence; thus, the targeted mutation results in a knockout of OMP (Potter *et al*, 2001). OMP-GFP/GC-G-KO mice (with GFP-labeled GG neurons lacking functional GC-G) were obtained by crossing GC-G-KO and OMP-GFP mice as described previously (Chao *et al*, 2015). Mice were kept on a standard 12-h light/dark cycle. All experimental procedures were approved by the Institutional Animal Care and Utilization Committee at Academia Sinica (Taiwan).

Calcium imaging

Calcium imaging experiments were performed as detailed recently (Chao *et al*, 2015). In brief, HEK-293T cells were seeded on 30-mm

coverslips coated with poly-D-lysine and transfected with an expression plasmid encoding CNGA3 or together with an expression vector encoding GC-G fused to GFP for identification of transfected cells. Two days after transfection, cells were loaded with Fura-2AM (Invitrogen/Thermo Fisher Scientific, Waltham, MA, USA) and coverslips were placed in a POC open perfusion chamber (Pecon, Erbach, Germany) filled with warm (37°C) Ca^{2+} recording buffer (supplemented with 1 mM of the phosphodiesterase inhibitor IBMX) for 2 min prior to perfusion with SBT-containing recording buffer (supplemented with 1 mM IBMX). Images were acquired every 1 s. Results are expressed as the ratio of 340-nm to 380-nm (R340/380) signals.

For calcium imaging of GG coronal sections, we used newborn mice [postnatal days 1–4 (P1–P4)] to prepare coronal tissue slices (60–100 μm thick) of the GG. The tissue was loaded with 15 μM Fura-2/AM (Invitrogen/Thermo Fisher Scientific) for 1 h at room temperature in oxygenated solution. Slices were then placed in the bath chamber (RC-26; Warner Instruments, Hamden, CT, USA) and immobilized with a slice anchor. Subsequently, ratiometric Ca^{2+} imaging was performed as described previously (Schmid *et al*, 2010; Chao *et al*, 2015) using buffer solutions with a temperature of 37°C.

Innate fear behavior tests

In essence, behavioral tests were carried out as described recently (Brechbuhl *et al*, 2013b; Matsuo *et al*, 2015). Briefly, male mice (8–10 weeks old) were housed in isolated cages (one mouse per cage) 1 day before the experiments were carried out; 1 h prior to the onset of the behavioral tests, mice were transferred in their cages to the laboratory in which the experiments were performed. The ambient temperature was kept at 23°C. The experiments were conducted during the dark phase of a 12-h:12-h light/dark cycle; they were recorded using a HD camera prior to offline analyses utilizing TopScan (Clever Sys Reston, VA, USA) and FreezeScan (Clever Sys). Mice were familiarized with handling, the test arena (a closed box of 30 × 15 × 12 cm), and artificial cerebrospinal fluid [ACSF; 118 mM NaCl, 25 mM $NaHCO_3$, 10 mM D-glucose, 2 mM KCl, 2 mM $MgCl$, 1.2 mM NaH_2PO_4, and 2 mM $CaCl_2$ (pH 7.4)] presented to them on a piece of blotting paper (3 cm × 3 cm). Subsequently, animals were transferred to the test arena. The total walking distance, the duration of stay in area 1 and area 2 as well as the freezing time were determined in the presence or absence of 50 μl of 1% SBT (dissolved in DMSO). Animals were exposed only once to each tested stimulus (ACSF or SBT, respectively). Freezing was defined as the time in which mice were immobile and displayed only respiratory movements. For measuring the total walking distance, the freezing time and the duration of stay in area 1 and area 2, only the first 5 min of the session was analyzed. To assess the general olfactory capacity of the investigated mice, following a food deprivation of 24 h, an Oreo cookie was buried in the home cage of the animals under 1 cm of bedding and the time to find the cookie was determined. The location of the cookie was varied systematically. Experiments were performed on 3 consecutive days.

Serum corticosterone assay

To measure serum corticosterone concentrations, for exposure to ACSF as well as to SBT, six adult male mice were tested. Similar to

the behavioral tests described above, mice were housed in isolated cages (one mouse per cage) 1 day prior to the experiments; 1 h before to the onset of the behavioral tests, mice were transferred in their cages to the laboratory in which the experiments were carried out. The ambient temperature was kept at 23°C. The experiments were conducted during the dark phase of a 12-h:12-h light/dark cycle. In brief, following exposure to 50 μl of 1% SBT or ACSF (applied on a piece of blotting paper) for 5 min, cervical dislocation was performed and blood was collected from the inferior vena cava. Similar to a recent study (Brechbuhl *et al*, 2013b), blood samples were subsequently centrifuged at room temperature for 5 min at 10,000 *g* and stored at −80°C until further analyses were conducted utilizing the Corticosterone ELISA kit (Enzo Life Sciences, Farmingdale, NY, USA). Corticosterone concentrations were determined in duplicate according to the protocol of the manufacturer.

Blood pressure measurement

The blood pressure of mice was determined utilizing a BP-2000 Blood Pressure Analysis System (Visitech Systems, Apex, NC, USA), a rapid and non-invasive tail-cuff approach. Essentially, the procedure of blood pressure measurement was performed as described in a recent report (Brechbuhl *et al*, 2015). In brief, during five consecutive days, adult mice (8 weeks old) were habituated to the experimental procedure, the investigator, and the technical equipment. The animals were held on the tail-cuff platform (heated to 37°C) by magnetic restrainers. To examine the effect of SBT on blood pressure, 50 μl of ACSF or 1% SBT was deposited on a piece of blotting paper (3 × 3 cm) and placed in front of the test mice without any physical contact. First, a measuring session was performed in which only the blotting paper was presented to the animals. Then, the blood pressure was measured continuously starting with three control session (exposure to ACSF) followed by three sessions with SBT. Each session comprised 10 successive measurements. The systolic and diastolic pressures were determined by the BP-2000 Analysis Software (Visitech Systems).

Statistical analyses

Values are expressed as mean ± SD. For the serum corticosterone assay, blood pressure measurement, and the behavioral experiments, *P*-values were determined by two-tailed paired *t*-test (with 95% confidence interval). In Fig 4D, SBT-induced ΔR (ratio of fluorescence intensity) was analyzed by two-tail unpaired *t*-test. Significance levels are indicated as follows: *$P < 0.05$; **$P < 0.01$.

Expanded View for this article is available online.

Author contributions

Y-CC, JF, and R-BY designed research. Y-CC performed research. Y-CC, JF, and R-BY analyzed data. Y-CC, JF, and R-BY wrote the manuscript.

Conflict of interest

The authors declare that they have no conflict of interest.

References

Arakawa H, Kelliher KR, Zufall F, Munger SD (2013) The receptor guanylyl cyclase type D (GC-D) ligand uroguanylin promotes the acquisition of food preferences in mice. *Chem Senses* 38: 391–397

Brauchi S, Orta G, Salazar M, Rosenmann E, Latorre R (2006) A hot-sensing cold receptor: C-terminal domain determines thermosensation in transient receptor potential channels. *J Neurosci* 26: 4835–4840

Brechbuhl J, Klaey M, Broillet MC (2008) Grueneberg ganglion cells mediate alarm pheromone detection in mice. *Science* 321: 1092–1095

Brechbuhl J, Moine F, Broillet MC (2013a) Mouse Grueneberg ganglion neurons share molecular and functional features with *C. elegans* amphid neurons. *Front Behav Neurosci* 7: 193

Brechbuhl J, Moine F, Klaey M, Nenniger-Tosato M, Hurni N, Sporkert F, Giroud C, Broillet MC (2013b) Mouse alarm pheromone shares structural similarity with predator scents. *Proc Natl Acad Sci USA* 110: 4762–4767

Brechbuhl J, Moine F, Tosato MN, Sporkert F, Broillet MC (2015) Identification of pyridine analogs as new predator-derived kairomones. *Front Neurosci* 9: 253

Chao YC, Cheng CJ, Hsieh HT, Lin CC, Chen CC, Yang RB (2010) Guanylate cyclase-G, expressed in the Grueneberg ganglion olfactory subsystem, is activated by bicarbonate. *Biochem J* 432: 267–273

Chao YC, Chen CC, Lin YC, Breer H, Fleischer J, Yang RB (2015) Receptor guanylyl cyclase-G is a novel thermosensory protein activated by cool temperatures. *EMBO J* 34: 294–306

Chu R, Reczek D, Brondyk W (2014) Capture-stabilize approach for membrane protein SPR assays. *Sci Rep* 4: 7360

Duda T, Sharma RK (2008) ONE-GC membrane guanylate cyclase, a trimodal odorant signal transducer. *Biochem Biophys Res Commun* 367: 440–445

Farah VM, Joaquim LF, Bernatova I, Morris M (2004) Acute and chronic stress influence blood pressure variability in mice. *Physiol Behav* 83: 135–142

Fleischer J, Schwarzenbacher K, Besser S, Hass N, Breer H (2006) Olfactory receptors and signalling elements in the Grueneberg ganglion. *J Neurochem* 98: 543–554

Fleischer J, Schwarzenbacher K, Breer H (2007) Expression of trace amine-associated receptors in the Grueneberg ganglion. *Chem Senses* 32: 623–631

Fleischer J, Breer H, Strotmann J (2009a) Mammalian olfactory receptors. *Front Cell Neurosci* 3: 9

Fleischer J, Mamasuew K, Breer H (2009b) Expression of cGMP signaling elements in the Grueneberg ganglion. *Histochem Cell Biol* 131: 75–88

Forte LR Jr (2004) Uroguanylin and guanylin peptides: pharmacology and experimental therapeutics. *Pharmacol Ther* 104: 137–162

Gruneberg H (1973) A ganglion probably belonging to the *N. terminalis* system in the nasal mucosa of the mouse. *Z Anat Entwicklungsgesch* 140: 39–52

Hanke W, Mamasuew K, Biel M, Yang RB, Fleischer J (2013) Odorant-evoked electrical responses in Grueneberg ganglion neurons rely on cGMP-associated signaling proteins. *Neurosci Lett* 539: 38–42

Hu J, Zhong C, Ding C, Chi Q, Walz A, Mombaerts P, Matsunami H, Luo M (2007) Detection of near-atmospheric concentrations of CO2 by an olfactory subsystem in the mouse. *Science* 317: 953–957

Jemiolo B, Alberts J, Sochinski-Wiggins S, Harvey S, Novotny M (1985) Behavioural and endocrine responses of female mice to synthetic analogues of volatile compounds in male urine. *Anim Behav* 33: 1114–1118

Kuhn M, Ng CK, Su YH, Kilic A, Mitko D, Bien-Ly N, Komuves LG, Yang RB (2004) Identification of an orphan guanylate cyclase receptor selectively expressed in mouse testis. *Biochem J* 379: 385–393

Kuhn M (2009) Function and dysfunction of mammalian membrane guanylyl cyclase receptors: lessons from genetic mouse models and implications for human diseases. *Handb Exp Pharmacol* 191: 47–69

Kuhn M (2016) Molecular physiology of membrane guanylyl cyclase receptors. *Physiol Rev* 96: 751–804

Lehman-McKeeman LD, Caudill D, Rodriguez PA, Eddy C (1998) 2-sec-butyl-4,5-dihydrothiazole is a ligand for mouse urinary protein and rat alpha 2u-globulin: physiological and toxicological relevance. *Toxicol Appl Pharmacol* 149: 32–40

Leinders-Zufall T, Cockerham RE, Michalakis S, Biel M, Garbers DL, Reed RR, Zufall F, Munger SD (2007) Contribution of the receptor guanylyl cyclase GC-D to chemosensory function in the olfactory epithelium. *Proc Natl Acad Sci USA* 104: 14507–14512

Lin H, Cheng CF, Hou HH, Lian WS, Chao YC, Ciou YY, Djoko B, Tsai MT, Cheng CJ, Yang RB (2008) Disruption of guanylyl cyclase-G protects against acute renal injury. *J Am Soc Nephrol* 19: 339–348

Liu CY, Fraser SE, Koos DS (2009) Grueneberg ganglion olfactory subsystem employs a cGMP signaling pathway. *J Comp Neurol* 516: 36–48

Mamasuew K, Breer H, Fleischer J (2008) Grueneberg ganglion neurons respond to cool ambient temperatures. *Eur J Neurosci* 28: 1775–1785

Mamasuew K, Hofmann N, Breer H, Fleischer J (2011a) Grueneberg ganglion neurons are activated by a defined set of odorants. *Chem Senses* 36: 271–282

Mamasuew K, Hofmann N, Kretzschmann V, Biel M, Yang RB, Breer H, Fleischer J (2011b) Chemo- and thermosensory responsiveness of Grueneberg ganglion neurons relies on cyclic guanosine monophosphate signaling elements. *Neuro-Signals* 19: 198–209

Matsuo T, Hattori T, Asaba A, Inoue N, Kanomata N, Kikusui T, Kobayakawa R, Kobayakawa K (2015) Genetic dissection of pheromone processing reveals main olfactory system-mediated social behaviors in mice. *Proc Natl Acad Sci USA* 112: E311–E320

Moss RL, Flynn RE, Shi J, Shen XM, Dudley C, Zhou A, Novotny M (1998) Electrophysiological and biochemical responses of mouse vomeronasal receptor cells to urine-derived compounds: possible mechanism of action. *Chem Senses* 23: 483–489

Munger SD, Leinders-Zufall T, McDougall LM, Cockerham RE, Schmid A, Wandernoth P, Wennemuth G, Biel M, Zufall F, Kelliher KR (2010) An olfactory subsystem that detects carbon disulfide and mediates food-related social learning. *Curr Biol* 20: 1438–1444

Novotny M, Harvey S, Jemiolo B, Alberts J (1985) Synthetic pheromones that promote inter-male aggression in mice. *Proc Natl Acad Sci USA* 82: 2059–2061

Papalia GA, Leavitt S, Bynum MA, Katsamba PS, Wilton R, Qiu H, Steukers M, Wang S, Bindu L, Phogat S, Giannetti AM, Ryan TE, Pudlak VA, Matusiewicz K, Michelson KM, Nowakowski A, Pham-Baginski A, Brooks J, Tieman BC, Bruce BD *et al* (2006) Comparative analysis of 10 small molecules binding to carbonic anhydrase II by different investigators using Biacore technology. *Anal Biochem* 359: 94 – 105

Potter SM, Zheng C, Koos DS, Feinstein P, Fraser SE, Mombaerts P (2001) Structure and emergence of specific olfactory glomeruli in the mouse. *J Neurosci* 21: 9713 – 9723

Potter LR (2011) Guanylyl cyclase structure, function and regulation. *Cell Signal* 23: 1921 – 1926

Schmid A, Pyrski M, Biel M, Leinders-Zufall T, Zufall F (2010) Grueneberg ganglion neurons are finely tuned cold sensors. *J Neurosci* 30: 7563 – 7568

Schwende FJ, Wiesler D, Jorgenson JW, Carmack M, Novotny M (1986) Urinary volatile constituents of the house mouse, Mus musculus, and their endocrine dependency. *J Chem Ecol* 12: 277 – 296

Spehr M, Spehr J, Ukhanov K, Kelliher KR, Leinders-Zufall T, Zufall F (2006) Parallel processing of social signals by the mammalian main and accessory olfactory systems. *Cell Mol Life Sci* 63: 1476 – 1484

Spehr M, Munger SD (2009) Olfactory receptors: G protein-coupled receptors and beyond. *J Neurochem* 109: 1570 – 1583

Takahashi LK (2014) Olfactory systems and neural circuits that modulate predator odor fear. *Front Behav Neurosci* 8: 72

Valentino MA, Lin JE, Snook AE, Li P, Kim GW, Marszalowicz G, Magee MS, Hyslop T, Schulz S, Waldman SA (2011) A uroguanylin-GUCY2C endocrine axis regulates feeding in mice. *J Clin Invest* 121: 3578 – 3588

Vay L, Gu C, McNaughton PA (2012) The thermo-TRP ion channel family: properties and therapeutic implications. *Br J Pharmacol* 165: 787 – 801

Yang J, Wang X, Fuh G, Yu L, Wakshull E, Khosraviani M, Day ES, Demeule B, Liu J, Shire SJ, Ferrara N, Yadav S (2014) Comparison of binding characteristics and *in vitro* activities of three inhibitors of vascular endothelial growth factor A. *Mol Pharm* 11: 3421 – 3430

Zhou A, Moss RL (1997) Effect of urine-derived compounds on cAMP accumulation in mouse vomeronasal cells. *NeuroReport* 8: 2173 – 2177